Bioresource Technology 403 (2024) 130849

Contents lists available at ScienceDirect

Bioresource Technology

journal homepage: www.elsevier.com/locate/biortech

Distinctive effects of graphene oxide and reduced graphene oxide on methane production kinetics and pharmaceuticals removal in anaerobic reactors

Oriol Casabella-Font [a,b,*], Massimiliano Riva [a,c], Jose Luis Balcázar [a,b], Jelena Radjenovic [a,d], Maite Pijuan [a,b,*]

[a] Catalan Institute for Water Research (ICRA), C. Emili Grahit 101, 17003 Girona, Spain
[b] Universitat de Girona, Girona, Spain
[c] University of Insubria, Como, Italy
[d] Catalan Institution for Research and Advanced Studies (ICREA), Passeig Lluís Companys 23, 08010, Barcelona, Spain

HIGHLIGHTS

- Biologically reduced graphene oxide enhances the methane production rate by 37%.
- Bio- and h-reduced graphene oxide methane kinetics were not statistically different.
- Graphene oxide addition affects the removal of pharmaceuticals.
- Bio- or h-reduced graphene oxide does not enhance the removal of pharmaceuticals.
- The addition of graphene oxide impacts the expression of functional genes.

GRAPHICAL ABSTRACT

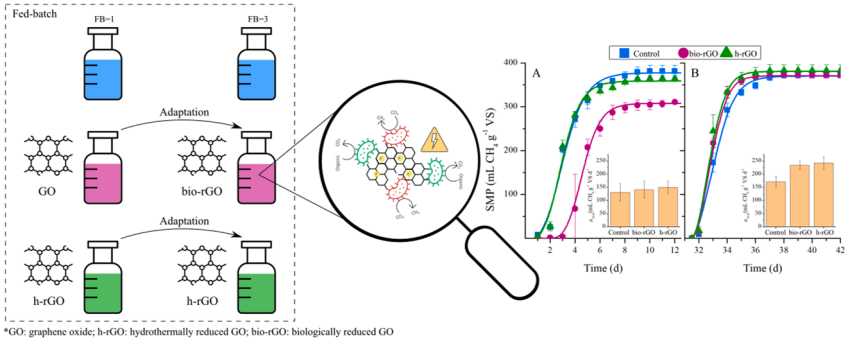

*GO: graphene oxide; h-rGO: hydrothermally reduced GO; bio-rGO: biologically reduced GO

ARTICLE INFO

Keywords:
Anaerobic biotransformation
Bio-reduced graphene oxide
Direct interspecies electron transfer
Methanogenesis
Micropollutants

ABSTRACT

Graphene oxide (GO) addition to anaerobic digestion has been suggested to enhance direct electron transfer. The impact of GO (0.075 g GO g^{-1} VS) and biologically and hydrothermally reduced GO (bio-rGO and h-rGO, respectively) on the methane production kinetics and removal of 12 pharmaceuticals was assessed in Fed-batch reactors. A decrease of 15 % in methane production was observed in the tests with GO addition compared with the control and the h-rGO. However, bio-rGO and h-rGO substantially increased the methane production rate compared to the control tests (+40 %), in the third fed-batch test. Removal of pharmaceuticals was enhanced only during the bio-reduction of GO (1st fed-batch test), whereas once the GO was bio-reduced, it followed a similar trend in the control and h-rGO tests. The addition of GO can enhance the methane production rate and, therefore, reduce the anaerobic treatment time.

* Corresponding authors.
E-mail addresses: ocasabella@icra.cat (O. Casabella-Font), mpijuan@icra.cat (M. Pijuan).

https://doi.org/10.1016/j.biortech.2024.130849
Received 15 March 2024; Received in revised form 13 May 2024; Accepted 14 May 2024
Available online 15 May 2024

1. Introduction

Anaerobic wastewater treatment is considered an alternative to conventional aerobic treatment. This process consists of four steps in which complex organic matter is transformed into methane, i.e., hydrolysis, acetogenesis, acidogenesis, and methanogenesis. Hydrolysis is the limiting step of the entire process since it is necessary to release extracellular enzymes (i.e., cellulases, proteinases, and lipases) to break up the macromolecular structures (Chandra et al., 2012; Vavilin et al., 2008). Besides hydrolysis, methanogenesis is the subsequent critical step that has a direct effect on the methane production kinetics (Dong et al., 2019; Kato et al., 2012).

The microbiome of anaerobic sludge is composed of a consortium of microorganisms, each with different roles in the different steps. Thus, interspecies communication is essential for the stability of the process. The synergetic relationship between anaerobic microorganisms is responsible for different biological reactions, often resulting in low process kinetic rates leading to high retention times (Wu et al., 2020). Interspecies electron transfer (IET) is the primary limitation of the anaerobic processes since it is conducted through molecules that are released into the mixed liquor (Luo et al., 2020; Zhong et al., 2022). Alternatively, electrons can be exchanged through physical structures (e.g., conductive material, and conductive pili) in a direct interspecies electron transfer (DIET), thus overcoming the mass transfer limitations associated with the usage of the dissolved biomolecules. Syntrophic bacteria live on the metabolic by-products produced by other microorganisms. The first evidence of DIET was published by Summers et al. (2010), after observing the electron exchange in cellular aggregates. Previous studies reported the impact of carbon-based conductive materials, e.g. granular activated carbon (GAC), biochar, and graphene, to promote the electron exchange through a conductive material (Lin et al., 2017; Luo et al., 2020). For example, the addition of 15 g L^{-1} of GAC to anaerobic batch reactors enhanced the methane production by 45 % in the co-digestion of waste-activated sludge and food waste (Johnravindar et al., 2020). Other studies have focused on the graphene-based materials such as graphene oxide (GO), which is biologically reduced under anaerobic conditions to conductive reduced graphene oxide (bio-rGO). It was observed that loadings of 50–500 mg GO L^{-1} negatively affected the methane production and kinetic rate, reducing the specific methane production by 10–20 %, whereas a loading of 5 mg/L did not significantly decrease the methane production (Colunga et al., 2015; Dong et al., 2019; Zhang et al., 2017). A recent study used the fed-batch (FB) strategy to monitor the impact of GO (<25 mg GO g^{-1} volatile solids (VS)) on methane production during five sequential batch tests, and reported that the total methane production was recovered after one feed step (Ponzelli et al., 2022a). Therefore, anaerobic biomass seems to require an adaptation period to GO, initially affecting its methane production, but recovering after GO is incorporated into the sludge.

Besides methane production, many efforts are focused on the occurrence and removal of emerging contaminants during anaerobic wastewater treatment (Ponzelli et al., 2022b; Zahedi et al., 2022). Anaerobic biodegradation of organic pollutants depends on the functional groups present in their molecular structure, making some of them very persistent to biological transformation (Ghattas et al., 2017). However, the addition of conductive materials can enhance their biodegradability (Liu et al., 2012). A previous study reported a 3.5-fold increase in the removal rate of azo dyes (i.e., reactive red 2 and 3-chloronitrobenzene) under methanogenic conditions by adding 5 mg GO L^{-1} (Colunga et al., 2015). Similarly, nitrobenzene biotransformation was enhanced after amending anaerobic sludge with 150 mg GO L^{-1} (Wang et al., 2014). Moreover, the addition of GO has been recently reported to enhance the overall removal of a wide range of pharmaceuticals (e.g., carbamazepine, sulfamethoxazole, roxithromycin) (Casabella-Font et al., 2023b). However, the impact of GO on the removal rates was not monitored.

The objective of this study was to assess the adaptation of the anaerobic sludge to GO, i.e., the formation of bio-rGO, focusing on the effect of GO on the methane production and removal of pharmaceuticals. We investigated the impact of GO addition at 0.075 g GO g^{-1} VS concentration on the methane production kinetics, both during the early exposure of the anaerobic biomass to GO, as well as after the adaptation of the biomass to (r)GO using a FB strategy. Upon addition, GO is rapidly bio-reduced to bio-rGO. The results were compared with the experiments run with the addition of hydrothermally reduced GO (h-rGO). Furthermore, pharmaceuticalś removal by the anaerobic microbial community was assessed during the initial exposure with GO and h-rGO, and after three sequential batch tests.

2. Materials and methods

2.1. Reagents and inoculum source

The anaerobic sludge (AnS) used as inoculum was collected from an anaerobic digester that treats waste activated sludge in Girona's municipal wastewater treatment plant (Catalonia, Spain). Microcrystalline cellulose was used as substrate following the protocol published by Anaerobic Digestion Specialist Group of the International Water Association (IWA) (Holliger et al., 2016), and was purchased from Sigma Aldrich (Sigma Aldrich Inc., USA). All standards used for the micropollutants stock solution and calibration curve were of analytical grade and purchased from Sigma Aldrich (USA) and Toronto Research Chemicals (Canada). GO was purchased from Graphenea (Spain) as 0.4 % w/w aqueous dispersion (>95 % of purity) with a monolayer size lower than 10 μm. Hydrothermally reduced graphene oxide (h-rGO) dispersion (0.4 % w/w) was prepared using a hydrothermal process (180 °C for 12 h) using 0.4 % GO solution as a stock solution. Characterization of graphene-based materials is provided in Supplementary Material (Baptista-Pires et al., 2021).

2.2. Analytical methods

Analyses of total solids (TS) and volatile solids (VS) were performed following the Standard Methods (APHA 2017). Target pharmaceuticals were analyzed using ultra-high performance liquid chromatography (UHPLC) (Waters Corporation, MA, USA) in tandem with a 5500 QTRAP hybrid quadrupole-linear ion trap tandem mass spectrometer (AB Sciex, Foster City, USA). Details of the analytical method are summarized in previous studies (Gros et al., 2019).

2.3. Biochemical methane potential tests

2.3.1. Non-adapted sludge biochemical methane potential tests

Biochemical methane potential (BMP) tests were set up in 600 mL glass bottles, using an inoculum to substrate ratio of two (in VS) (Zahedi et al., 2018). Methane production was monitored online using a Gas Endeavour instrument (Bioprocess Control, Sweden). The equipment had incorporated a scrubber solution with 3 N NaOH to remove acid compounds from the biogas produced. High-precision methane production data was collected using 2 mL flow cells with a range of measurement of 0.2 to 1500 mL h^{-1}. To assess the removal of pharmaceuticals, another set of BMPs was prepared by sealing the bottles with a rubber stopper, which allowed sampling while keeping the bottles airtight and under anaerobic conditions. Two mL of mixed liquor was centrifuged at 11,000 g for 10 min. The supernatant was filtered through 0.22 μm polyvinylidene difluoride (PVDF) filters and kept at −20 °C until the analysis. To ensure anaerobic environment, the headspace was flushed with pure N_2 for two min. A mix of target pharmaceuticals, namely two macrolides (i.e., azithromycin (AZM) and roxithromycin (ROX)), two tetracyclines (i.e., tetracycline (TTC) and chlortetracycline (CTC)), two sulfonamides (i.e., sulfamethoxazole (SMX) and sulfadiazine (SDZ)), three fluoroquinolones (i.e., enrofloxacin (ENO), norfloxacin (NOR), and ofloxacin (OFX)), trimethoprim

(TMP), carbamazepine (CBZ), and iohexol (IHX). The selected pharmaceuticals are representative of four widely used families of antibiotics (i.e., macrolides, fluoroquinolones, tetracyclines, and sulfonamides), and include also CBZ and IHX, both highly persistent to biological treatment, thus leading to their frequent detection in the environment. Target pharmaceuticals were added to achieve initial concentrations of 1 μM each by adding 25 μL of concentrated standard solutions (1/4, v/v, methanol/water). Abiotic transformations and adsorption of pharmaceuticals onto GO and/or microcrystalline cellulose was investigated in a separate set of experiments, in the presence of the same amounts of substrate (1.09 g), pharmaceuticals, and GO/h-rGO (40 mL 0.4 % GO) used in the biotic experiments (with inoculum), but replacing the inoculum with water.

Three tests were conducted in triplicate: *i)* control (AnS) without GO or h-rGO (Control); *ii)* addition of 0.075 g GO g^{-1} VS (AnS + GO); and *iii)* addition of 0.075 g h-rGO g^{-1} VS (AnS + rGO). GO and h-rGO were added according to the VS content of the inoculum. This GO concentration was chosen according to a previous study that reported an enhancement in the removal of pharmaceuticals in the anaerobic digestion of waste-activated sludge (Casabella-Font et al., 2023b).

2.3.2. Fed-batch biochemical methane potential tests

The second set of BMP tests was prepared with new/fresh inoculum to study the impact of the addition of GO and h-rGO in midterm conditions (45 days). A fed-batch (FB) strategy was employed to assess the adaptation of the anaerobic sludge to both graphene-based materials, e.g., to bio-rGO formation in the case of GO addition. A single dose of GO or h-rGO was added at the beginning, while three doses of cellulose (1.09 g cellulose each) were added on day 0, day 15, and day 30, resulting in three sets of consecutive tests: FB1, FB2, and FB3. An extra dose of microcrystalline cellulose for the subsequent sequential batches (FB2 and FB3) was added after achieving a daily methane production of < 1 mL d^{-1}. The removal of pharmaceuticals was monitored in FB3. The same conditions were assessed in triplicate: *i)* control without adding GO/h-rGO (Control_FB); *ii)* addition of 0.075 g GO g^{-1} VS; (GO_FB); *iii)* addition of 0.075 g h-rGO g^{-1} VS (h-rGO_FB). GO and h-rGO were added according to the VS content of the inoculum.

2.4. Experimental data modeling

To describe and compare quantitatively the experimental data on the methane production, we used the Gompertz mathematical model (Eq. (1), a modified sigmoidal curve previously reported to describe methane production of simple substrates degradation with an initial lag-phase (Ware and Power, 2017). The Excel solver function estimated three different parameters by fitting the experimental data and the theoretical model using minimum squared error methodology. Each parameter was represented in the model as follows: *i)* maximum specific methane production (mL CH_4 g^{-1} VS) as M_∞; *ii)* maximum methane production rate (mL CH_4 g^{-1} VS d^{-1}) as μ_{max}; *iii)* lag phase as λ (days). To evaluate the statistical differences between data, ANOVA tests were carried out using Minitab 17 Statistical Software (State College, PA: Minitab, Inc.).

$$M(t) = M_\infty \cdot e\left\{ -e\cdot\left[\frac{\mu_{max}\cdot e}{M_\infty}\cdot(\lambda - t) + 1 \right] \right\} \quad (1)$$

2.5. 16S and functional gene expression characterization

RNeasy PowerBiofilm kit (QIAGEN, NL) was used to extract the total RNA from the microbial samples. High-throughput sequencing of the extracted RNA was then performed using the NovaSeq 6000 platform (Illumina Inc., San Diego, CA). The extraction was done from the control and GO conditions at different times of the non-adapted sludge experiments, i.e., after 24 and 72 h for the control, and after 72 h for the GO. In order to characterize the taxonomic composition of the metatranscriptomic dataset, reads were aligned against the NCBI non-redundant (NR) protein database (https://ftp.ncbi.nlm.nih.gov/blast/db/FASTA/nr.gz, April 2023) using DIAMOND (version 2.1.6) with default parameters (Buchfink et al., 2014). The lowest common ancestor approach implemented in MEGAN6 was used to assign reads at the phylum level (Huson et al., 2016). Aligned reads were also assigned to the hierarchical subsystems based on the KEGG database (Kanehisa et al., 2016). The relative abundance of genes was determined by RPKM for normalization (Xia et al., 2023). Data was deposited in the NCBI BioProject database under the access number PRJNA1097379.

3. Results and discussion

3.1. Impact of GO and h-rGO on the methane production

Fig. 1 illustrates the impact of two graphene-based materials (GO and h-rGO) on the methane production kinetics and the control condition without the addition of any nanomaterial. The Gompertz model equation (Eq. (1)) was fitted to the experimental specific methane production (SMP) obtained to estimate the kinetic parameters that describe the methane production, allowing a quantitative comparison between the studied conditions. The results were presented as means with the standard deviation of each determined parameter (Table 1) and grouped according to the result of the statistical analysis. The maximum specific methane production (M_∞) obtained in the presence of h-rGO was 365 ± 5 mL CH_4 g^{-1} VS, showing no significant statistical differences with the Control (374 ± 12 mL CH_4 g^{-1} VS). Thus, the addition of h-rGO had no impact on the methane production during the anaerobic digestion of cellulose. This finding differs from the previous studies that reported an enhanced methane production of complex substrates such as cattle manure and organic fraction of municipal waste with the addition of rGO (Gökçek et al., 2021; Muratçobanoğlu et al., 2021). Contrary to h-rGO, the addition of GO significantly reduced the M_∞ by ~ 15 % (Table 1), resulting in SMP of 315 ± 21 mL CH_4 g^{-1} VS. Negative effect of GO addition on the SMP was also reported during the anaerobic digestion of waste-activated sludge (Casabella-Font et al., 2023b; Dong et al., 2019). The principal hypothesis was that a fraction of the available electrons in the substrate was scavenged by the GO reduction and

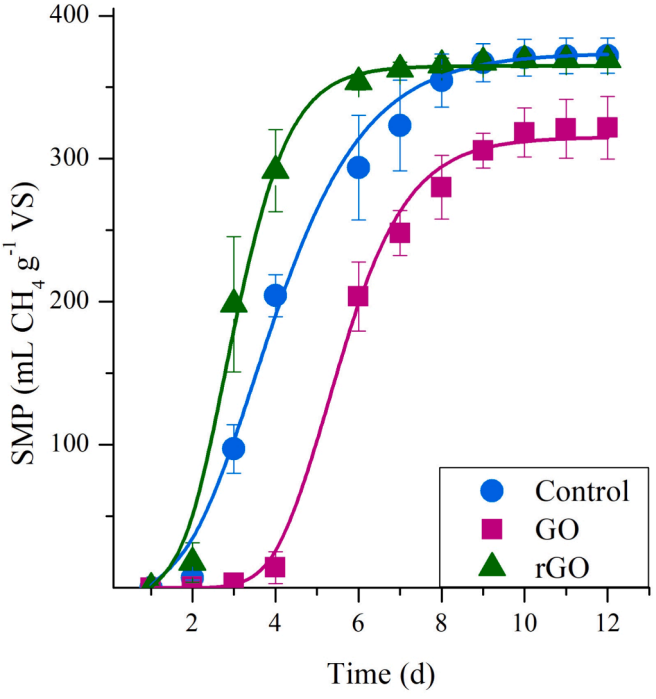

Fig. 1. Experimental specific methane production (SMP) for each condition tested (symbols) and Gompertz model curve (lines).

Table 1
Summary of the kinetic parameters that fit the Gompertz model to experimental specific methane potential expressed as means and standard deviation for the three conditions tested.

Code	M_o (mL CH_4 g^{-1} VS)	μ_{max} (mL CH_4 g^{-1} VS d^{-1})	λ (d)
Control	374 ± 12 ^{A}	80 ± 8 ^{A}	2.0 ± 0.3 ^{A}
GO	315 ± 21^{B}	115 ± 5 ^{A}	4.1 ± 0.6^{B}
h-rGO	365 ± 5 ^{A}	179 ± 40^{B}	1.9 ± 0.1 ^{A}

*R^2 was greater than 0.99 for the three conditions; ^{A} and ^{B} indicate statistical differences between conditions for the same parameter.

formation of bio-rGO. Indeed, previous study (Ponzelli et al., 2022b) demonstrated that the biological reduction of GO occurs during the first hours of exposure of the anaerobic sludge.

The maximum methane production rate (μ_{max}) was another parameter used to describe the methane production kinetics. In this case, a positive impact of the addition of both GO and h-rGO was detected. The μ_{max} was increased by ~ 40 % (GO) and ~ 120 % (h-rGO), compared with the maximum production rate obtained in the Control, with values of 115 ± 5 and 179 ± 40 mL CH_4 g^{-1} VS d^{-1}, respectively. However, further statistical tests revealed that only the data obtained for h-rGO was statistically different ($p < 0.05$) compared with the Control. On the other hand, the lag phase was increased by adding GO, being two times longer as compared with the Control and h-rGO conditions (Table 1), probably caused by the biological reduction of GO. The lower SMP but higher μ_{max}, as well as the prolonged lag phase, supported the hypothesis that the microorganisms use the substrate to reduce the GO at the beginning of the experiment, instead of completing the anaerobic digestion process by producing methane. Previous studies stated that the biological reduction of GO mediated by c-type cytochromes uses the oxygen functional groups in the GO structure as electron acceptors (Hua et al., 2023; Shen et al., 2018). Thus, a fraction of the substrate is used as electron donor to reduce the GO structure, resulting in a lower SMP due to the electron scavenging effect of the bio-reduction of GO.

After the first set of experiments, a fed-batch strategy was used to assess the mid-term impact of GO/h-rGO on the anaerobic digestion process using fresh sludge as inoculum but with the same GO/h-rGO concentration. This methodology allows to refeed the cultures to expand the experimental period. However, it should be considered that the substrate composition could compromise the microbiological activity due to the deficit of micro and macronutrients. Fig. 2A-C presents the maximum methane production rates obtained in each FB test, and methane production kinetics profiles. The three-step fed-batch process was divided into the first batch (FB1) (days 0–15), the second batch (FB2) (days 16–30), and the third batch (FB3) (days 30–45). During FB1, lower methane production was measured in the tests with addition of GO (GO_FB1; Table 2), compared with the other conditions evaluated, in agreement with the first set of experiments (Fig. 1). After statistical analysis, the SMP obtained in GO_FB1 and the other conditions in this period (Control_FB1 and h-rGO_FB1) were statistically different (Table 2). In this case, the SMP was reduced by ~ 22 % in comparison with the Control_FB1, and ~ 16 % after the addition of h-rGO (h-rGO_FB1). Also, a prolonged lag phase was detected in the presence of GO (3.5 ± 0.5 d) at the beginning of the experiment, compared with Control_FB1 and h-rGO_FB1 (1.6 ± 0.2 d and 1.7 ± 0.2 d, respectively). Concerning the maximum specific methane production rates, no significant differences were detected between the three conditions (Control_FB1, GO_FB1, and h-rGO_FB1), showing values ~ 140 mL CH_4 g^{-1} VS d^{-1} (Fig. 2C, Table 2). After achieving a daily methane production of < 1 mL d^{-1}, a second dose of microcrystalline cellulose was added to the microcosmos for the subsequent sequential batches (FB2 and FB3). Compared with the FB1, a shorter lag phase (1 day) was detected for the three conditions (Table 2). The SMP obtained in FB2 and FB3 were not statistically different compared to the Control_FB1 and h-rGO_FB1. This confirms that the addition of GO only inhibits the methane production

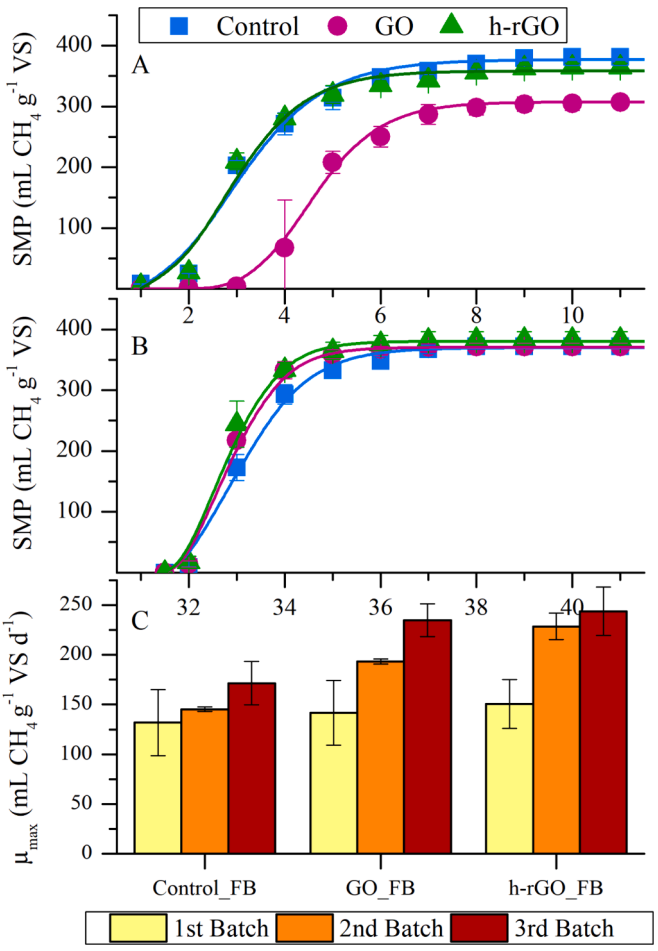

Fig. 2. (A) Experimental specific methane production (SMP) during the first batch (0–15 d) for each condition assessed (symbols) and Gompertz model curve (lines). (B) SMP during the third batch (30–45 d). (C) Specific methane production rates (μmax) obtained in the different sequential batches in the presence of GO and h-rGO, and without (Control), using a fed-batch strategy. Statistical differences are summarized in Supplementary Material.

Table 2
Kinetic parameters that describe the specific methane production by fitting the Gompertz model to the experimental data obtained in the different sequential batches. The results are expressed as the mean and standard deviation.

Name	M_o (mL CH_4 g^{-1} VS)	μ_{max} (mL CH_4 g^{-1} VS d^{-1})	λ (d)
Control_FB1	377 ± 14 ^{A}	131 ± 33 ^{A}	1.6 ± 0.2 ^{A}
GO_FB1	307 ± 6^{B}	141 ± 32 ^{A}	3.5 ± 0.5^{B}
h-rGO_FB1	358 ± 5 ^{A}	150 ± 24 ^{AB}	1.7 ± 0.2 ^{A}
Control_FB2	377 ± 8 ^{A}	145 ± 2 ^{A}	1.0 ± 0.1 ^{A}
GO_FB2	359 ± 3 ^{A}	193 ± 2 ^{ABCD}	1.0 ± 0.1 ^{A}
h-rGO_FB2	360 ± 9 ^{A}	228 ± 13 ^{BCD}	1.1 ± 0.1 ^{A}
Control_FB3	369 ± 5 ^{A}	171 ± 21 ^{AB}	1.0 ± 0.1 ^{A}
GO_FB3	370 ± 5 ^{A}	234 ± 16^{CD}	1.1 ± 0.1 ^{A}
h-rGO_FB3	380 ± 12 ^{A}	243 ± 24 ^{D}	1.0 ± 0.1 ^{A}

R^2 was greater than 0.99 for the three conditions; ^{ABCD} indicate statistical differences between conditions for the same parameter.

during the first exposure of the anaerobic biomass to the nanomaterial, and that the total methane production is not increased by the addition of GO/rGO.

The addition of GO/h-rGO had a positive impact on the specific methane production rate. μ_{max} significantly increased in the tests that contained GO and h-rGO and also between the first (FB1) and second (FB2) batches. Since the production rate was kept constant in different

Control tests, the methane production rate enhancement obtained after the addition of GO/h-rGO was associated with an increase of the electron exchange flux in the presence of both graphene-based materials. However, there was no direct evidence of DIET except for the higher methane production rate. No significant statistical differences were detected between the second (FB2) and the third (FB3) tests.

The results obtained in the second set of experiments confirm that the addition of GO led to electron scavenging, causing a prolonged lag phase and lower specific methane production in FB1. After the GO was reduced by the anaerobic microbial community, methane production rate increased by ~ 37 % compared with the Control ($p > 0.05$) during FB3, showing equivalent results as h-rGO (Fig. 2).

The results obtained differ from the ones reported in the literature. A previous study by Ponzelli et al., (2022a) investigated the impact of GO on methane production. The experiments were conducted using GO concentrations between 0.005–0.025 g GO g VS^{-1} and reported that the addition of GO did not enhance the maximum specific methane production rate using the same standard substrate (i.e., cellulose). Although

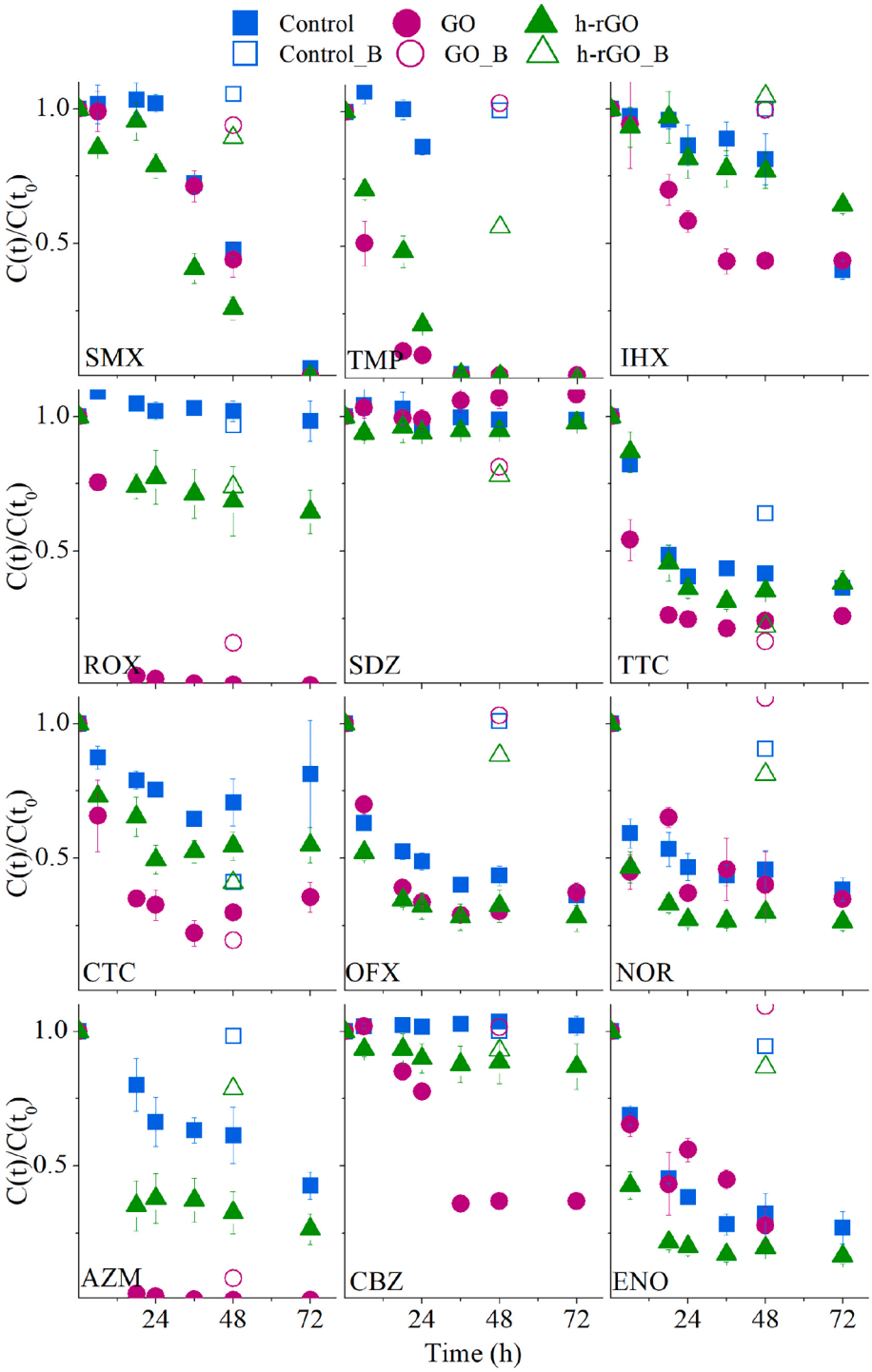

Fig. 3. Removal profiles for the different pharmaceuticals in presence of GO (purple circle), h-rGO (green triangle), and Control (blue square). Abiotic tests are represented in hollow symbols with the same colors. Results are presented as concentration measured at time t (Ct) normalized to the initial concentration (C0) (1 μM).

the authors report an enhancement of the specific methane production rate when glucose was added, the hydrolysis step was not involved in the process. In the present study, the GO concentration was 3.75-fold higher and positively impacted the maximum methane production rate using cellulose as carbon source. Enhancing the methane production kinetics with the addition of GO implies a faster degradation of complex organic matter, accelerating the reaction rate of the limiting steps. Thus, the addition of both graphene-based materials studied may be considered as an opportunity to improve the performance of anaerobic digesters and enable the treatment of higher organic loads with smaller reactors.

3.2. Impact of GO and h-rGO on the removal of pharmaceuticals

The impact of GO and h-rGO on the biological removal of twelve pharmaceuticals was assessed with fresh inoculum sludge (non-adapted to GO/h-rGO) and compared with the GO/h-rGO adapted sludges obtained in the GO_FB3 and h-rGO_FB3 conditions. Biotransformation and adsorption on the GO/h-rGO were considered as possible removal mechanisms. The removal of pharmaceuticals caused by abiotic factors was assessed after 48 h in the tests without inoculum. Fig. 3 presents the removal of pharmaceuticals obtained with the non-adapted sludge, and in the abiotic tests.

TTC and CTC were adsorbed onto the GO/h-rGO to a significant degree (i.e., 84 % and 78 % removal, respectively), which can be justified by their molecular structure rich in double bonds and aromatic rings, which promotes π-π interactions and hydrogen bonds (Ai et al., 2019; Gao et al., 2012; Ghadim et al., 2013). Moreover, both antibiotics were also adsorbed onto cellulose, with 40 % and 60 % removal observed after 48 h, respectively. Previous studies also reported tetracyclines removal by adsorption onto microcrystalline cellulose and GO (Amaly et al., 2022; Li et al., 2017; Sun et al., 2021).

Macrolides ROX and AZM were significantly adsorbed onto GO, resulting in a removal of ~ 85 %. In the abiotic test with h-rGO, the achieved removals were ~ 25 %. The concentration of ROX remained unchanged in both the Control and abiotic tests with cellulose, indicating that abiotic transformations or adsorption did not occur. AZM removal was 39 ± 10 % after 48 h, and 57 ± 5 % after 72 h in the Control test, attributed to its biotransformation given that it was not removed in the abiotic control test with cellulose. In the presence of GO/h-rGO, ROX presented similar behavior in the abiotic controls and tests with anaerobic sludge, suggesting that it was removed more due to adsorption onto the conductive material rather than due to biotransformation. Thus, the main removal mechanism of ROX was adsorption onto the GO/h-rGO structure, whereas AZM was biodegraded.

OFX, NOR, and ENO did not show significant differences between the control, the GO and the h-rGO tests, and their removal was 65–75 %. Since the three antibiotics presented the highest removals in the presence of anaerobic sludge, their removal could be attributed to biotransformation. Although the overall achieved removal was similar between the studied conditions, the removal of OFX and NOR was enhanced in the presence of both GO and h-rGO.

The concentration of SMX decreased until reaching complete removal by the end of the experiment in all three conditions tested. TMP biotransformation was highly influenced by the addition of GO and h-rGO, with removals of 90 ± 2 % and 79 ± 2 %, respectively, after the first 24 h, significantly higher compared with the Control in which TMP removal was 13 ± 3 % after 24 h. TMP was completely removed in the presence of GO and h-rGO in 36 h. The concentration of SDZ remained constant in any of the conditions tested, indicating that this pharmaceutical was neither biotransformed nor adsorbed onto the biomass.

Abiotic experiments showed no adsorption of IHX onto GO/rGO. The removal of IHX in the Control and with the added h-rGO was 20 % in the first 36 h, whereas in the case GO the observed removal of IHX was 60 %. By the end of the test, the removal of IHX in the presence of GO was comparable to that obtained in the Control tests. In the presence of h-rGO, the removal profile was similar to the Control, but achieved an overall removal of < 40 %. The differences in the removal suggested that the removal of IHX in the presence of GO might follow a different metabolic pathway than the Control.

CBZ had the highest removal enhancement by the addition of GO compared to other pharmaceuticals. CBZ concentrations remained unchanged in the Control experiment, whereas its removal in the presence of h-rGO was 10 ± 5 % in the first 24 h and remained unchanged until the end of the experiment (i.e., 13 ± 8 %). On the other hand, in the presence of GO, 22 ± 1 % of CBZ removal was observed after 24 h and was enhanced to up to 63 ± 1 % after 40 h, which represented an enhancement of ~ 50 % as compared with the h-rGO test. CBZ removal can be associated with biological transformation since CBZ concentration remained constant in the abiotic conditions measured after 48 h. Previous studies reported that CBZ was poorly removed or recalcitrant during anaerobic digestion (Carballa et al., 2006; Malmborg and Magnér, 2015; Narumiya et al., 2013). However, in a previous study, 57 % of CBZ removal was observed during the anaerobic digestion of waste-activated sludge with the same concentration of GO (Casabella-Font et al., 2023b).

The addition of GO induces modifications in both the sludge matrix and the microbial communities, fostering the proliferation of phylogenetic groups that could benefit from the presence of a conductive material (Casabella-Font et al., 2023a, 2023b). These studies observed the adaptation of the microbial consortium to the presence of GO, and the subsequent impact on the removal of pharmaceuticals during the anaerobic digestion process of municipal wastewater and waste-activated sludge. In the present study, the results obtained after FB3 tests allowed us to assess the impact of the adaptation to the conductive material on the removal of pharmaceuticals (See Supplementary Material).

CBZ was the pharmaceutical that presented the highest enhancement in its removal by the addition of GO in FB1. However, after the adaptation period, the anaerobic sludge (both GO_FB3 and h-rGO_FB3) exhibited the same behavior as the control condition, with hardly any CBZ removal. This result suggests that the higher removal of CBZ observed in FB1 was related with the biological reduction of GO.

Previously, adaptation of the anaerobic consortium to the conductive materials (GO and h-rGO) enhanced the removal of fluoroquinolone antibiotics (OFX, NOR, and ENO) (Casabella-Font et al., 2023b). Contrary to what was expected, in this study fluoroquinolone antibiotics showed a lower removal percentage by the end of the experiment and exhibited similar removal profiles to the Control experiments without the presence of (r)GO. Since GO and h-rGO were incorporated into the sludge matrix, it was not possible to investigate the adsorption of antibiotics onto these nanomaterials while excluding biotransformation.

SMX and TMP had similar removal, showing no difference between the control and the GO/h-rGO tests, in contrast with the previous study where the removal of these two compounds was enhanced by the addition of GO during the operation of an anaerobic membrane bioreactor amended with GO (0.005–0.1 g GO g^{-1} VS) (Casabella-Font et al., 2023a). The adaptation of microorganisms to the conductive materials did not have an impact on the removal of SDZ, for which the removal remained below 5 %.

After the adaptation to GO/h-rGO, IHX presented a sharp decrease in concentration. However, both conductive materials negatively affected the removal of IHX in comparison to the Control. In the Control IHX was completely removed within 48 h, whereas in GO_FB3 and h-rGO_FB3 IHX was ~ 90 % removed after 72 h. As was observed in the case of CBZ, IHX profiles suggest that the removal of this pharmaceutical is enhanced during the biological reduction of GO.

Tetracyclines (TTC and CTC) exhibited very different behavior with the sludges adapted to GO/h-rGO. Neither TTC nor CTC were removed in any condition (See Supplementary Material). Different conditions presented similar profiles, suggesting that the GO/h-rGO material is incorporated into the sludge structure, and the removal of both antibiotics during the FB1 was due to adsorption onto the graphene-based

materials.

Although the sludges adapted to GO and h-rGO did not present enhanced removal of ROX and AZM (See Supplementary Material), these results also supported the hypothesis of the GO incorporation into the sludge matrix, given that neither of the two macrolides was eliminated in the presence of GO after the adaptation period (GO_FB3). Contrary to what was previously reported during the operation of an anaerobic membrane bioreactor (Casabella-Font et al., 2023a), ROX removal was not enhanced by the presence of bio-rGO.

Overall, although it was expected that the addition of GO/h-rGO would enhance the removal of the pharmaceuticals under anaerobic conditions by the promotion of DIET, the removal was not enhanced after the adaptation of the sludge to both graphene-based materials for any of the pharmaceuticals. The lower removals observed after the adaptation of sludge to the conductive material may be caused by different phenomena, for example, changes in the microbial community. Furthermore, as observed in the case of CBZ and IHX, biological reduction of GO (and h-rGO) can impact the biotransformation of organic contaminants because of the stress response of the microbial community, and/or due to the expression of specific enzymes.

Previous studies reported that adding GO enhances the overall removal of pharmaceuticals (i.e., from both liquid and solid phase) during anaerobic digestion of waste-activated sludge (Casabella-Font et al., 2023b). Likewise, the removal of azo and nitroaromatic dyes was also reported in a synthetic medium under methanogenic conditions (Colunga et al., 2015). According to the results presented in this study, the pharmaceutical removal under methanogenic conditions was only improved when GO was added and no enhancement was observed after this GO was biologically reduced.

It is worth noting that the methane production results (see section 3.1) demonstrate that GO enhances the anaerobic digestion kinetics, accelerating the methane production rate, supporting the hypothesis that GO promotes the DIET phenomena once it is biologically reduced, but it negatively affects the methane production kinetics during the firsts 72–96 h (longer lag-phase). Conversely, the results assessing the impact of GO did not show differences between conditions, although differences were detected using non-adapted sludge and GO. Specifically, CBZ and IHX presented higher removals in the presence of GO during the first batch test, which were attributed to biotransformation since there was no removal due to their adsorption. Nevertheless, during the test using adapted anaerobic sludge, CBZ concentration remained unchanged, and IHX presented better results with the sludge that did not contain GO/h-rGO. Thus, enhanced removal of pharmaceuticals was likely not due to bio-rGO enhanced DIET, but due to the stress response of the microbial community caused by the addition of GO.

3.3. Impact of graphene oxide on genes expression levels

Expression of functional genes quantified by sequencing the extracted RNA samples was assessed after 24 and 72 h in the control condition,

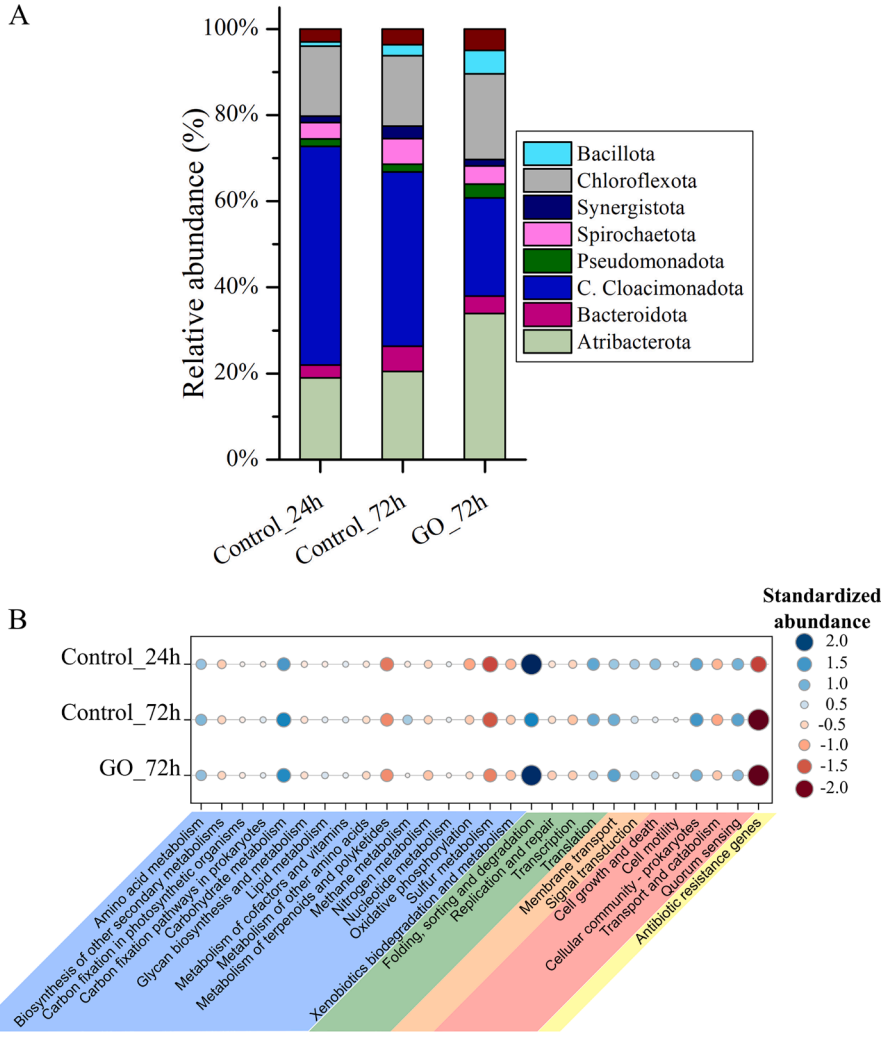

Fig. 4. Metatranscriptomic analysis. (A) Taxonomic annotation at phylum level according to 16S gene expression. (B) Functional gene expression at different times in the presence of 0.075 g GO g^{-1} VS and in the control, whose values are normalized among different times based on Z-score.

as well as in the presence of GO after 72 h. The dataset was aligned against the NCBI non-redundant (NR) protein database and the taxonomic annotation at phylum level is shown in Fig. 4A. The expression of the 16S gene showed that Candidatus Cloacimonadota (51 %) was the most active phylum in the control condition, followed by Atribacterota (19 %) and Chloroflexota (formerly Chloroflexi or green nonsulfur bacteria) (16 %). These phyla are known as the dominants in anaerobic digesters (Kim et al., 2022; Kirkegaard et al., 2017). Other active phyla represented less than 5 % at this point of the experiment. After 72 h of experiment, bacteria affiliated to the Candidatus Cloacimonadota phylum were less active, representing 40 % in the control, and 23 % in the presence of GO. At this point, the Atribacterota phylum benefited from the GO addition, increasing their relative activity (34 %), and remained constant in the control condition when comparing both sampling times. Members belonging to the Chloroflexota phylum were also promoted by the addition of GO, increasing their relative activity (20 %) compared to the control (16 %) at 72 h. Spirochaetota (formerly Spirochaetes) and Bacteroidota (formerly Bacteroidetes) doubled their relative activity in the absence of GO, whereas GO addition did not change. Bacteria affiliated to Bacillota (formerly Firmicutes) was the less active phylum in the control at 24 h, representing ~ 1 %. However, their activity increased in both conditions after 72 h, representing more than 5 % in the presence of GO. A recent study on the impact of GO on the microbial community under anaerobic conditions revealed that Bacillota and Chloroflexota were promoted by the addition of GO, increasing their relative abundance in both cases. Furthermore, the relative abundance of Spirochaetota and Bacteroidota was reduced in the presence of GO (Casabella-Font et al., 2023b). A previous study suggested that some bacteria (i.e., *Clostridium* spp., *Bacillus* spp., and *Syntrophomonas* spp.,) have potential electrogenic ability, all of them surprisingly belonging to the Bacillota phylum (Park et al., 2018). Electrogenic microorganisms are those which can benefit from the presence of GO, taking advantage of the DIET phenomena.

Expressed functional genes were classified according to the KEGG database (Fig. 4B). Among the genes classified in the *metabolism* category, a similar expression was determined concerning carbohydrate metabolism, which includes the glycolysis pathway to oxidase glucose. Although the methane production was negatively affected during the early contact with GO (see section 3.1), the substrate was degraded, supporting the previously stated hypothesis that part of the substrate electrons was used to reduce the GO. Moreover, the genes responsible for methane production (i.e., the autoclastic and hydrogenotrophic pathways) were under-expressed in the presence of GO at 72 h in comparison with the control at 72 h, confirming the hypothesis that the substrate did not complete the anaerobic digestion process and it is used as the electron donor for the bioreduction of GO.

GO could cause a cellular oxidative stress response, thus inhibiting the microbial activity (Goodarzi et al., 2024). In this study, we aimed to assess the expression of functional genes related to the stress response. Concerning the genes classified in the *genetic information processing* category, expression of genes classified in the *folding, sorting, and degradation* group (according to KEGG database) were overexpressed in GO at 72 h. The twin-arginine translocation (Tat) pathway is a protein transport system that transports folded proteins (e.g., anaerobic respiration, osmotic stress defense, and biofilm formation) from the cytoplasm to the membrane of bacteria and archaea microorganisms. Among the different proteins that could be translocated to the membrane, some of them could be associated with the stress response. The combination of Tat system and peroxidases showed to be the key combination to oxidative stress on a facultative anaerobic microorganism (Ochsner et al., 2002; Zhang et al., 2015). The overexpression of the Tat system might be related to the stress caused by the presence of GO and may also be related to the formation of an observed hydrogel. Although the 12 antibiotics (i.e., fluoroquinolones, sulfonamides, macrolides, tetracyclines, among others) were spiked at 1 μM, the expression of antibiotic resistance genes decreased after 72 h in both conditions, in comparison with the initial expression observed in the control at 24 h. Further research is needed to identify the proteins associated with the biological reduction of GO and that are also responsible for the transformation of pharmaceuticals.

4. Conclusions

The addition of GO and h-rGO distinctively impacted the methane production and the removal of pharmaceuticals during anaerobic digestion. Initially, GO inhibits methane production. However, after GO bio-reduction, the kinetic rates increase by ~ 37 %. The removal of the pharmaceuticals is enhanced with the addition of GO/h-rGO, mainly due to adsorption. However, the removal of CBZ and IHX is enhanced during the initial bioreduction of GO. After the sludge adaptation to bio-rGO/h-rGO, the removal of CBZ and IHX is not affected by the presence of bio-rGO/h-rGO, suggesting the key role of GO bioreduction on the enhancement of their anaerobic biotransformation.

CRediT authorship contribution statement

Oriol Casabella-Font: Writing – original draft, Visualization, Methodology, Investigation, Data curation, Conceptualization. **Massimiliano Riva:** Investigation. **Jose Luis Balcázar:** Visualization, Data curation. **Jelena Radjenovic:** Writing – review & editing, Supervision, Resources, Project administration, Methodology, Funding acquisition. **Maite Pijuan:** Writing – review & editing, Supervision, Resources, Project administration, Methodology, Funding acquisition.

Declaration of competing interest

The authors declare that they have no known competing financial interests or personal relationships that could have appeared to influence the work reported in this paper.

Data availability

Data will be made available on request.

Acknowledgments

This research is funded by AEI (Agencia Estatal de Investigación, Spanish Government) through project ANTARES (PID2019-110346RB-C22). O. Casabella-Font acknowledges funding from Secretariat of Universities and Research from Generalitat de Catalunya and European Social Fund for his FI fellowship (2023 FI-3 00122). The authors acknowledge the support from the Economy and Knowledge Department of the Catalan Government through a Consolidated Research Group (ICRA-TECH - 2021 SGR 01283). We also acknowledge the support from Fundació I-CERCA through the CERCAGINYS program, funded by the Ministerio de Ciencia e Innovación (MICINN, Spanish Government)

Appendix A. Supplementary data

Supplementary data to this article can be found online at https://doi.org/10.1016/j.biortech.2024.130849.

References

Ai, Y., Liu, Y., Huo, Y., Zhao, C., Sun, L., Han, B., Cao, X., Wang, X., 2019. Insights into the adsorption mechanism and dynamic behavior of tetracycline antibiotics on reduced graphene oxide (RGO) and graphene oxide (GO) materials. Environ. Sci. Nano 6, 3336–3348. https://doi.org/10.1039/c9en00866g.

Amaly, N., EL-Moghazy, A.Y., Nitin, N., Sun, G., Pandey, P.K., 2022. Synergistic adsorption-photocatalytic degradation of tetracycline by microcrystalline cellulose composite aerogel dopped with montmorillonite hosted methylene blue. Chem. Eng. J. 430, 133077. https://doi.org/10.1016/j.cej.2021.133077.

Baptista-Pires, L., Norra, G.F., Radjenovic, J., 2021. Graphene-based sponges for electrochemical degradation of persistent organic contaminants. Water Res. 203, 117492 https://doi.org/10.1016/j.watres.2021.117492.
Buchfink, B., Xie, C., Huson, D.H., 2014. Fast and sensitive protein alignment using DIAMOND. Nat. Methods 12, 59–60. https://doi.org/10.1038/nmeth.3176.
Carballa, M., Omil, F., Alder, A.C., Lema, J.M., 2006. Comparison between the conventional anaerobic digestion of sewage sludge and its combination with a chemical or thermal pre-treatment concerning the removal of pharmaceuticals and personal care products. Water Sci. Technol. 53, 109–117. https://doi.org/10.2166/wst.2006.241.
Casabella-Font, O., Ponzelli, M., Papapanou, M., Balcazar, J.L., Pijuan, M., Radjenovic, J., 2023a. Impact of graphene oxide addition on pharmaceuticals removal in anaerobic membrane bioreactor. Bioresour. Technol. 383, 129252 https://doi.org/10.1016/j.biortech.2023.129252.
Casabella-Font, O., Zahedi, S., Gros, M., Luis, J., Radjenovic, J., Pijuan, M., 2023b. Graphene oxide addition to anaerobic digestion of waste activated sludge : Impact on methane production and removal of emerging contaminants. Environ. Pollut. 324, 121343 https://doi.org/10.1016/j.envpol.2023.121343.
Chandra, R., Takeuchi, H., Hasegawa, T., 2012. Methane production from lignocellulosic agricultural crop wastes: A review in context to second generation of biofuel production. Renew. Sustain. Energy Rev. 16, 1462–1476. https://doi.org/10.1016/j.rser.2011.11.035.
Colunga, A., Rangel-Mendez, J.R., Celis, L.B., Cervantes, F.J., 2015. Graphene oxide as electron shuttle for increased redox conversion of contaminants under methanogenic and sulfate-reducing conditions. Bioresour. Technol. 175, 309–314. https://doi.org/10.1016/j.biortech.2014.10.101.
Dong, B., Xia, Z., Sun, J., Dai, X., Chen, X., Ni, B.J., 2019. The inhibitory impacts of nano-graphene oxide on methane production from waste activated sludge in anaerobic digestion. Sci. Total Environ. 646, 1376–1384. https://doi.org/10.1016/j.scitotenv.2018.07.424.
Gao, Y., Li, Y., Zhang, L., Huang, H., Hu, J., Shah, S.M., Su, X., 2012. Adsorption and removal of tetracycline antibiotics from aqueous solution by graphene oxide. J. Colloid Interface Sci. 368, 540–546. https://doi.org/10.1016/j.jcis.2011.11.015.
Ghadim, E.E., Manouchehri, F., Soleimani, G., Hosseini, H., Kimiagar, S., Nafisi, S., 2013. Adsorption properties of tetracycline onto graphene oxide: Equilibrium, kinetic and thermodynamic studies. PLoS One 8, 1–9. https://doi.org/10.1371/journal.pone.0079254.
Ghattas, A., Fischer, F., Wick, A., Ternes, T.A., 2017. Anaerobic biodegradation of (emerging) organic contaminants in the aquatic environment. Water Res. 116, 268–295. https://doi.org/10.1016/j.watres.2017.02.001.
Gökçek, Ö.B., Muratçobanoğlu, F., Muratçobanoğlu, H., Uçar, D., Mert, R.A., Yıldırım, B., Zan, R., Demirel, S., 2021. The effect of reduced graphene oxide addition on methane production from municipal organic solid waste. J. Chem. Technol. Biotechnol. 96, 2845–2851. https://doi.org/10.1002/jctb.6835.
Goodarzi, M., Arjmand, M., Eskicioglu, C., 2024. Insight into anaerobic digestion mechanisms by fine-tuning structural properties of nanomaterial supplements. Chem. Eng. J. 483, 149256 https://doi.org/10.1016/j.cej.2024.149256.
Gros, M., Marti, E., Balcázar, J.L., Boy-Roura, M., Busquets, A., Colón, J., Sànchez-Melsió, A., Lekunberri, I., Borrego, C.M., Ponsá, S., Petrovic, M., 2019. Fate of pharmaceuticals and antibiotic resistance genes in a full-scale on-farm livestock waste treatment plant. J. Hazard. Mater. 378, 120716 https://doi.org/10.1016/j.jhazmat.2019.05.109.
Holliger, C., Alves, M., Andrade, D., Angelidaki, I., Astals, S., Baier, U., Bougrier, C., Buffière, P., Carballa, M., De Wilde, V., Ebertseder, F., Fernández, B., Ficara, E., Fotidis, I., Frigon, J.C., De Laclos, H.F., Ghasimi, D.S.M., Hack, G., Hartel, M., Heerenklage, J., Horvath, I.S., Jenicek, P., Koch, K., Krautwald, J., Lizasoain, J., Liu, J., Mosberger, L., Nistor, M., Oechsner, H., Oliveira, J.V., Paterson, M., Pauss, A., Pommier, S., Porqueddu, I., Raposo, F., Ribeiro, T., Pfund, F.R., Strömberg, S., Torrijos, M., Van Eekert, M., Van Lier, J., Wedwitschka, H., Wierinck, I., 2016. Towards a standardization of biomethane potential tests. Water Sci. Technol. 74, 2515–2522. https://doi.org/10.2166/wst.2016.336.
Hua, Z., Tang, L., Wu, M., Fu, J., 2023. Graphene hydrogel improves S. putrefaciens' biological treatment of dye wastewater: Impacts of extracellular electron transfer and function of c-type cytochromes. Environ. Res. 236, 116739 https://doi.org/10.1016/j.envres.2023.116739.
Huson, D.H., Beier, S., Flade, I., Górska, A., El-Hadidi, M., Mitra, S., Ruscheweyh, H.J., Tappu, R., 2016. MEGAN Community Edition - Interactive Exploration and Analysis of Large-Scale Microbiome Sequencing Data. PLoS Comput. Biol. 12, 1–12. https://doi.org/10.1371/journal.pcbi.1004957.
Johnravindar, D., Liang, B., Fu, R., Luo, G., Meruvu, H., Yang, S., Yuan, B., Fei, Q., 2020. Supplementing granular activated carbon for enhanced methane production in anaerobic co-digestion of post-consumer substrates. Biomass and Bioenergy 136, 105543. https://doi.org/10.1016/j.biombioe.2020.105543.
Kanehisa, M., Sato, Y., Kawashima, M., Furumichi, M., Tanabe, M., 2016. KEGG as a reference resource for gene and protein annotation. Nucleic Acids Res. 44, D457–D462. https://doi.org/10.1093/nar/gkv1070.
Kato, S., Hashimoto, K., Watanabe, K., 2012. Methanogenesis facilitated by electric syntrophy via (semi)conductive iron-oxide minerals. Environ. Microbiol. 14, 1646–1654. https://doi.org/10.1111/j.1462-2920.2011.02611.x.
Kim, N.K., Lee, S.H., Kim, Y., Park, H.D., 2022. Current understanding and perspectives in anaerobic digestion based on genome-resolved metagenomic approaches. Bioresour. Technol. 344, 126350 https://doi.org/10.1016/j.biortech.2021.126350.
Kirkegaard, R.H., McIlroy, S.J., Kristensen, J.M., Nierychlo, M., Karst, S.M., Dueholm, M. S., Albertsen, M., Nielsen, P.H., 2017. The impact of immigration on microbial community composition in full-scale anaerobic digesters. Sci. Rep. 7, 1–11. https://doi.org/10.1038/s41598-017-09303-0.
Li, M. fang, Liu, Y. guo, Zeng, G. ming, Liu, S. bo, Hu, X. jiang, Shu, D., Jiang, L. hua, Tan, X. fei, Cai, X. xi, Yan, Z. li, 2017. Tetracycline absorbed onto nitrilotriacetic acid-functionalized magnetic graphene oxide: Influencing factors and uptake mechanism. J. Colloid Interface Sci. 485, 269–279. https://doi.org/10.1016/j.jcis.2016.09.037.
Lin, R., Cheng, J., Zhang, J., Zhou, J., Cen, K., Murphy, J.D., 2017. Boosting biomethane yield and production rate with graphene: The potential of direct interspecies electron transfer in anaerobic digestion. Bioresour. Technol. 239, 345–352. https://doi.org/10.1016/j.biortech.2017.05.017.
Liu, F., Rotaru, A.E., Shrestha, P.M., Malvankar, N.S., Nevin, K.P., Lovley, D.R., 2012. Promoting direct interspecies electron transfer with activated carbon. Energy Environ. Sci. 5, 8982–8989. https://doi.org/10.1039/c2ee22459c.
Luo, J., Zhang, Q., Zhao, J., Wu, Y., Wu, L., Li, H., Tang, M., Sun, Y., Guo, W., Feng, Q., Cao, J., Wang, D., 2020. Potential influences of exogenous pollutants occurred in waste activated sludge on anaerobic digestion: A review. J. Hazard. Mater. 383, 121176 https://doi.org/10.1016/j.jhazmat.2019.121176.
Malmborg, J., Magnér, J., 2015. Pharmaceutical residues in sewage sludge: Effect of sanitization and anaerobic digestion. J. Environ. Manage. 153, 1–10. https://doi.org/10.1016/j.jenvman.2015.01.041.
Muratçobanoğlu, H., Gökçek, Ö.B., Mert, R.A., Zan, R., Demirel, S., 2021. The impact of reduced graphene oxide (rGO) supplementation on cattle manure anaerobic digestion: Focusing on process performance and microbial syntrophy. Biochem. Eng. J. 173, 108080 https://doi.org/10.1016/j.bej.2021.108080.
Narumiya, M., Nakada, N., Yamashita, N., Tanaka, H., 2013. Phase distribution and removal of pharmaceuticals and personal care products during anaerobic sludge digestion. J. Hazard. Mater. 260, 305–312. https://doi.org/10.1016/j.jhazmat.2013.05.032.
Ochsner, U.A., Snyder, A., Vasil, A.I., Vasil, M.L., 2002. Effects of the twin-arginine translocase on secretion of virulence factors, stress response, and pathogenesis. Proc. Natl. Acad. Sci. u. s. a. 99, 8312–8317. https://doi.org/10.1073/pnas.082238299.
Park, J.H., Park, J.H., Je Seong, H., Sul, W.J., Jin, K.H., Park, H.D., 2018. Metagenomic insight into methanogenic reactors promoting direct interspecies electron transfer via granular activated carbon. Bioresour. Technol. 259, 414–422. https://doi.org/10.1016/j.biortech.2018.03.050.
Ponzelli, M., Radjenovic, J., Drewes, J.E., Koch, K., 2022a. Enhanced methane production kinetics by graphene oxide in fed-batch tests. Bioresour. Technol. 360, 127642 https://doi.org/10.1016/j.biortech.2022.127642.
Ponzelli, M., Zahedi, S., Koch, K., Drewes, J.E., Radjenovic, J., 2022b. Rapid biological reduction of graphene oxide: Impact on methane production and micropollutant transformation. J. Environ. Chem. Eng. 10, 108373 https://doi.org/10.1016/j.jece.2022.108373.
Shen, L., Jin, Z., Wang, D., Wang, Y., Lu, Y., 2018. Enhance wastewater biological treatment through the bacteria induced graphene oxide hydrogel. Chemosphere 190, 201–210. https://doi.org/10.1016/j.chemosphere.2017.09.105.
Summers, Z.M., Fogarty, H.E., Leang, C., Franks, A.E., Malvankar, N.S., Lovley, D.R., 2010. Direct Exchange of Electrons Within Aggregates of an Evolved Syntrophic Coculture of Anaerobic Bacteria. Science 80-.). 330, 1413–1415. https://doi.org/10.1126/science.1194472.
Sun, J., Cui, L., Gao, Y., He, Y., Liu, H., Huang, Z., 2021. Environmental application of magnetic cellulose derived from Pennisetum sinese Roxb for efficient tetracycline removal. Carbohydr. Polym. 251, 117004 https://doi.org/10.1016/j.carbpol.2020.117004.
Vavilin, V.A., Fernandez, B., Palatsi, J., Flotats, X., 2008. Hydrolysis kinetics in anaerobic degradation of particulate organic material: An overview. Waste Manag. 28, 939–951. https://doi.org/10.1016/j.wasman.2007.03.028.
Wang, J., Wang, D., Liu, G., Jin, R., Lu, H., 2014. Enhanced nitrobenzene biotransformation by graphene-anaerobic sludge composite. J. Chem. Technol. Biotechnol. 89, 750–755. https://doi.org/10.1002/jctb.4182.
Ware, A., Power, N., 2017. Modelling methane production kinetics of complex poultry slaughterhouse wastes using sigmoidal growth functions. Renew. Energy 104, 50–59. https://doi.org/10.1016/j.renene.2016.11.045.
Wu, Y., Wang, S., Liang, D., Li, N., 2020. Conductive materials in anaerobic digestion: From mechanism to application. Bioresour. Technol. 298, 122430 https://doi.org/10.1016/j.biortech.2019.122403.
Xia, R., Sun, M., Balcázar, J.L., Yu, P., Hu, F., Alvarez, P.J.J., 2023. Benzo[a]pyrene stress impacts adaptive strategies and ecological functions of earthworm intestinal viromes. ISME J. 1–11 https://doi.org/10.1038/s41396-023-01408-x.
Zahedi, S., Romero-Güiza, M., Icaran, P., Yuan, Z., Pijuan, M., 2018. Optimization of free nitrous acid pre-treatment on waste activated sludge. Bioresour. Technol. 252, 216–220. https://doi.org/10.1016/j.biortech.2017.12.090.
Zahedi, S., Gros, M., Casabella, O., Petrovic, M., Balcazar, J.L., Pijuan, M., 2022. Occurrence of veterinary drugs and resistance genes during anaerobic digestion of poultry and cattle manures. Sci. Total Environ. 822, 153477 https://doi.org/10.1016/j.scitotenv.2022.153477.
Zhang, J., Wang, Z., Wang, Y., Zhong, H., Sui, Q., Zhang, C., Wei, Y., 2017. Effects of graphene oxide on the performance, microbial community dynamics and antibiotic resistance genes reduction during anaerobic digestion of swine manure. Bioresour. Technol. 245, 850–859. https://doi.org/10.1016/j.biortech.2017.08.217.
Zhang, C., Xin, Y., Wang, Y., Guo, T., Lu, S., Kong, J., 2015. Identification of a novel dye-decolorizing peroxidase, efeB, translocated by a twin-arginine translocation system in streptococcus thermophilus CGMCC 7.179. Appl. Environ. Microbiol. 81, 6108–6119. https://doi.org/10.1128/AEM.01300-15.
Zhong, Y., He, J., Wu, F., Zhang, P., Zou, X., Pan, X., Zhang, J., 2022. Metagenomic analysis reveals the size effect of magnetite on anaerobic digestion of waste activated sludge after thermal hydrolysis pretreatment. Sci. Total Environ. 851, 158133 https://doi.org/10.1016/j.scitotenv.2022.158133.